Nanotoxicology

ISSN: 1743-5390 (Print) 1743-5404 (Online) Journal homepage: http://www.tandfonline.com/loi/inan20

Comparative modeling of exposure to airborne nanoparticles released by consumer spray products

Christian Riebeling, Andreas Luch & Mario Enrico Götz

To cite this article: Christian Riebeling, Andreas Luch & Mario Enrico Götz (2016) Comparative modeling of exposure to airborne nanoparticles released by consumer spray products, Nanotoxicology, 10:3, 343-351, DOI: 10.3109/17435390.2015.1071446

To link to this article: http://dx.doi.org/10.3109/17435390.2015.1071446

http://informahealthcare.com/nan
ISSN: 1743-5390 (print), 1743-5404 (electronic)

Nanotoxicology

Nanotoxicology, 2016; 10(3): 343–351
 DOI: 10.3109/17435390.2015.1071446

Taylor & Francis
Taylor & Francis Group

ORIGINAL ARTICLE

Comparative modeling of exposure to airborne nanoparticles released by consumer spray products

Christian Riebeling, Andreas Luch, and Mario Enrico Götz

Department of Chemical and Product Safety, German Federal Institute for Risk Assessment (BfR), Berlin, Germany

Abstract

Consumer exposure to sprays containing nano-objects is a continuing concern as a potential health hazard. One potential hazard has been formulated in the overload hypothesis. It describes a volume fraction of the macrophages that is occupied by deposited nanoparticles that leads to reduced macrophage mobility. Subsequent chronic inflammation may then lead to severe health consequences including cancer. To calculate lung deposition of spherical particles, the Multiple-Path Particle Dosimetry (MPPD) model (ARA, Albuquerque, NM) provides different kinds of lung models and age settings. Using the MPPD v 2.11 software, we modeled several consumer-related exposure scenarios. Different body orientations and age groups were investigated. Moreover, a number of materials representing different densities were used, and the exposure calculated using MPPD is compared to the hazard derived from the overload hypothesis. Conditions leading to macrophage overload were found for exposures to high particle doses for prolonged times and repeated exposure. Such conditions are unlikely in the context of regular consumer exposure. The overload hypothesis assumes the particles to be inert and biopersistent, a condition that currently lacks a clear regulatory definition and is valid only for a few selected materials. Furthermore, because of material-specific effects and the possibility of surface adsorption of hazardous chemicals, nano-objects in propellant sprays remain of concern for consumer health.

Keywords

Consumer spray products, exposure modeling, nanoparticle, overload hypothesis

History

Received 9 March 2015
Revised 24 June 2015
Accepted 6 July 2015
Published online 16 September 2015

Introduction

Nanotechnology has revolutionized production processes and shows promise in many other areas. A number of products that are refined by nanotechnology or contain nano-objects have already entered the consumer market. The database of the ''Project on Emerging Nanotechnologies'' (http://www.nanotechproject.org) of the Woodrow Wilson International Center for Scholars of 2013 lists 1628 consumer products that claim the use of nanotechnology.

In Germany, a series of respiratory symptoms with about 153 cases, in the worst cases developing toxic pulmonary edema, occurred in 2006 (Pauluhn et al., 2008). In these five cases, the pulmonary edema was reversible within one hour after hospitalization (ER/ICU) without specific treatments. A connection was quickly established between the symptoms and two propellant-based sprays. However, no nanoparticles (NPs) were found in the primary products. Similar products had been on the market as pump sprays for several years with no adverse health effects reported (BfR, 2006). It was later understood that a change to the formulation had been introduced with the conversion from a pump spray to the propellant-based spray. Zinc-coated spray cans had been employed; and therefore, sodium borate had been added as an anticorrosive. A consequential correction of the pH of the solution due to this change in formulation led to precipitation of nano- and microscale particles over time. Semi-volatile silanes, the surfactant ingredient, likely adsorbed onto the particles and were transported deep into the lungs with the particles acting as a vehicle. The silane-coated borate particles were then assumed to be the likely cause of the respiratory symptoms. Even if the product did not contain intentionally produced nanomaterials, this incident reinforced the interest of the authorities to potential hazards that could result from nanomaterials in consumer products.

Exposure to NPs via the respiratory tract is considered as the most likely situation that could lead to hazardous effects for the consumer (Hagendorfer et al., 2010). This concern is partly owed to the large surface of the lung. In addition, NPs more easily penetrate into the alveoli of the lung than do larger particles. Moreover, the barrier separating gas phase and blood in the alveoli consists of surfactant and only a few cells. Transition into the bloodstream is therefore conceivable and has already been shown for various materials (Balasubramanian et al., 2013; Kendall & Holgate, 2012; Kreyling et al., 2014). In contrast, dermal penetration is considered negligible at least for healthy skin (Labouta & Schneider, 2013; Nohynek & Dufour, 2012), and oral intake of some nanoscale materials is already commonplace (Peters et al., 2012; Weir et al., 2012). So far, no regulatory

Correspondence: Dr Christian Riebeling, Department of Chemical and Product Safety, German Federal Institute for Risk Assessment (BfR), Max-Dohrn-Strasse 8-10, 10589 Berlin, Germany. Tel: +49-(0)30-18412 3118. Fax: +49-(0)30-18412 4741. E-mail: Christian.Riebeling@bfr.bund.de

relevant adverse effects of the oral ingestion of these materials have been reported (Lewinson et al., 1994; Martin, 2007; Skocaj et al., 2011).

Respiratory exposure by consumer products occurs mainly using sprays and powders. In addition, NPs bound in a matrix might be released during processing of products, such as sawing, sanding or grinding. However, NPs remain bound in the matrix, tooling of which typically yields larger particles (Gomez et al., 2014).

A number of studies have investigated the release of nanomaterials from consumer products. In most cases spray applications were examined; and silver was the most frequently used nanomaterial in the spray applications. An experimental setup for the measurement of NPs in sprays was described by Hagendorfer et al. (2010). Two different atomizers were used and the droplet size determined of an aqueous spray liquid containing silver NPs. The propellant spray generated droplets with diameters in the nanometer range, while the pump spray produced large droplets that fell to the bottom of the chamber without reaching the detector. A similar difference between pump and propellant spray was found investigating four commercial sprays (Lorenz et al., 2011). In one case, no particles were found in the aerosol although silver was present; and in a second spray zinc oxide NPs were found. The liquid of the third spray was free of NPs, but NPs were found in the aerosol. This was probably due to formation of NPs from polyacrylate during the spraying (Lorenz et al., 2011). Another experimental setup for the determination of NPs in sprays has been described by Chen et al. (2010). An antibacterial spray containing titania NPs was investigated. In the aerosol, liquid droplets in the nanometer range and NPs were found. The investigated spray was also tested on rats in a subsequent study of the same group (McKinney et al., 2012). In the highest dose, exposure resulted in increased respiratory rate, pneumonia and lung cell damage. However, exposures in this dose range are not expected for consumers (McKinney et al., 2012). Other studies found varying contents of NPs in sprays. Advertising the use of nanotechnology did not necessarily mean the presence of NPs, and a number of sprays without reference to nanotechnology contained NPs (Nazarenko et al., 2011, Quadros & Marr, 2011).

One study examined three powders that specified the use of nanotechnology and three without such a claim (Nazarenko et al., 2012a). One of the nanotechnology products contained no NPs as judged by electron microscopy. The five other powders exhibited NPs albeit in large agglomerates.

Due to a number of experimental observations, the concept of dust overloading of the lungs as an adverse effect developed. Morrow (1988) formulated the overload hypothesis for the rat lung. It postulates that the loading of alveolar macrophages of the rat with particles of a volume of 6% of the macrophage cell volume leads to a reduced macrophage mobility and consequently reduced lung clearance. Chronic loading with inert, non-cytotoxic particles under these conditions is presumed to lead to inflammation and ultimately tumorigenesis in the rat lung (Morrow, 1988).

For consumer exposure it is common to use models to quantitatively estimate an exposure level. As reasoned above we focus on respiratory exposure. The Multiple-Path Particle Dosimetry (MPPD; Anjilvel & Asgharian, 1995) model v2.11 (ARA, Albuquerque, NM) is based on complex, multi-path lung models for particle exposure. Using MPPD, internal exposure can be calculated in detail. The tool is able to model particle deposition and clearance in the rat and the human lung. Within MPPD, various lung models are available for humans. The model allows the quantification of the deposition in different lung areas and also of the uptake into alveolar macrophages. Importantly, a separate NP model is integrated into version v2.11 of MPPD that allows exposure estimations of spherical nano-sized objects. Furthermore, MPPD allows for different body orientations of the exposed body to the spray. Consumers comprise all population groups and therefore also include particularly sensitive or vulnerable groups, such as children, pregnant women and the chronically ill. These different populations have to be considered when the risks of nanotechnology are assessed for consumers. Therefore, we calculated the NP burden upon different exposure scenarios employing the different lung models of MPPD v2.11. We then compare our results to the overload hypothesis as a generalized adverse health effect of inhaled particles.

Methods

The Multiple-Path Particle Dosimetry model v2.11 (at http://www.ARA.com/select products > software > MPPD: last accessed 12 May 2015) was used. Various lung models for humans of adult and different ages are provided. In addition, MPPD allows for different body orientations of the exposed body to the spray. Furthermore, algorithms to calculate clearance from the lung are available. However, the current algorithm of MPPD v2.11 for clearance of particles of any size is considered to be insufficient (Kalberlah et al., 2011). As a worst-case scenario, clearance was disregarded in this assessment.

Here, several exposure scenarios typical to consumers were simulated exploiting the possibility in MPPD to employ different human lung models and body orientations. Two different but related lung models were used for the exposure scenarios. The Yeh-Schum 5-Lobe model is based on data by Yeh and Schum (1980). It characterizes individual airways at the level of the segmental bronchi. Within each lobe, the airways are described in a single-path manner. A separate symmetric tree represents each of the five lobes. This model was considered the most relevant lung model by Kalberlah et al. (2011). The Age-specific 5-Lobe model uses a dichotomous, branching, symmetric-tree single path model, but structurally different lung similar to that of the Yeh-Schum 5-Lobe lobar-specific model. It is based on the data of Mortensen et al. (1983, 1989). The size and structure of the tree is dependent upon the age of the child or young adult. Appropriate functional residual lung capacity (Altman & Dittmer Katz, 1971; Dunnill, 1962; Overton & Graham, 1989; Phalen et al., 1985), head volume (Hart et al., 1963; Overton & Graham, 1989), tidal volume (Hofmann, 1982), and breathing frequency (Hofmann, 1982) default values are linked with their respective ages. The respiratory tract, according to the model, comprises three different compartments. Here,''head'' includes nasopharyngeal and laryngeal as well as oral deposition since all our scenarios assume both nasal and oral inhalation (see below). The ''conducting airways'' denote the tracheobronchial tree excluding the alveoli which are accounted for by the ''alveolar region''.

The first scenario ''consumer, upright'' follows the recommendation of the ''Report on the biological plausibility of HEC [human-equivalent concentration] and MPPD'' for modeling a worker (Kalberlah et al., 2011), commissioned by the German Federal Institute for Occupational Safety and Health (BAuA). This scenario is based on the default values, which model an upright standing human at rest. Important exceptions are the respiratory rate, for which 19 breaths/min are assumed to be representative for light activity, the tidal volume, which is assumed to be 1000 ml, and the oronasal-normal augmenter breathing for light activity. These values were derived from typical scenarios used to calculate threshold limit values at BAuA (Kalberlah et al., 2011). Supplemental Table 1 lists all input parameters used. The scenario ''consumer, upright'' models an

adult in light activity, such as spraying on tiles in a bathroom with a large angle, so that bounce effects are ignored.

For the scenario ''consumer, leaning forward'' the ''Age-specific 5-Lobe'' lung model was used and the (maximum) age of 21 years employed. Default values were used with the exception of the body orientation, which was set to 45°, leaning forward, and as breathing scenario the oronasal-normal augmenter breathing was set (Supplemental Table 2). This scenario may model the use of a spray on a shoe.

The third exposure scenario ''bystander, child'' can be understood as a second person in the previous scenario. In this case, the ''Age-specific 5-Lobe'' lung model was used and the age was set to 3 years. All default values were accepted with the exception of oronasal-normal augmenter breathing (Supplemental Table 3). Here, a child is modeled that is standing next to one of the adults of the scenarios ''consumer, upright'' or ''consumer, leaning forward".

An infant lying on its back was modeled for the scenario ''infant, lying'', again employing the ''Age-specific 5-Lobe'' lung model. Here, the lowest possible age setting of three months was used and the body orientation is ''on back". To model a heavily agitated infant, an increased tidal volume and an increased respiratory rate together with oronasal mouth breathing was applied. A doubling of the respiratory flow rate compared to the default values [total lung capacity (TLC) = 43.98 ml, respiratory flow rate of 39 breaths/min × 0.0304 l tidal volume = 1.1856 l/min] was assumed. For this purpose, the respiratory rate was set to 60 breaths/min and the tidal volume was set to 39.52 ml (60 breaths/min × 0.03952 l tidal volume = 2.3712 l/min breathing flow rate) (Supplemental Table 4). The scenario ''infant, lying'' represents a heavily agitated infant lying on its back to whom a spray or powder is applied.

The selection of nanomaterials intended to cover a wide range of material densities while using data of actual NPs investigated during the nanoGEM project (Wohlleben et al., 2014). Nanomaterials of relatively low agglomeration tendency were chosen. Moreover, a dose of 1×10^6 particles/cm^3 is employed unless otherwise stated. At this concentration, a low degree of agglomeration can be assumed and thus the modeling should be specific for nanomaterials. Moreover, this dose is within the higher range found in several consumer sprays on the market (Chen et al., 2010; Lorenz et al., 2011). For calculations, we assumed that the spray liquid is an aqueous suspension of the NPs that is dispersed into nanoscale droplets using a propellant. Furthermore, it is assumed that the aqueous shell of NP-carrying droplets evaporates before entry into the airways. Therefore, the exposure models described in the following could also apply to the use of powders. For most models, silver, zirconia and silica NPs were used (Table 1), the properties for the pristine NPs were taken from data sheets available through the nanoGEM project (Wohlleben et al., 2014). The nanoGEM NPs are not intended for spray applications and no data on particle properties upon spraying was available. Thus, for most models, the average diameter was employed as count median diameter (CMD) with an assumed geometric standard deviation (GSD) of 1.5 (Table 1), similar to what has been achieved in dry generators for inhalation studies on rats (Sung et al., 2011). These parameters describe moderately polydispersed particles, corresponding to a low agglomeration status.

Here, GSD is the geometric standard deviation. The natural logarithm of the GSD($\ln(\sigma_g)$) is defined in MPPD as ''the standard deviation of $\ln(d)$, where d is the particle geometric diameter. $\ln(\sigma_g)$ is derived from the square root of the ratio of the 84th percentile diameter to the 16th percentile diameter. The aerosol is assumed to be monodispersed or a lognormally distributed polydispersed distribution if the value of the GSD is specified to be <1.05 or ≥ 1.05, respectively''.

In some cases two types of density were used, the physical density ρ of the material, and that of a ''loosest'' packing of spherical particles of $\rho_{wp} = {}^1/_6 \times \pi \times \rho$ (Table 1). These two densities represent the extreme range of material density, one for the solid material and one for agglomerates, which are composed of spheres in cubic lattice packing. The equation does not compensate for liquid filling the voids, thus accounting for imperfect packing.

Results

To understand the particle size dependency of deposition after inhalation exposure, we investigated two different aerosol concentrations and three different particle sizes in the exposure scenario ''consumer, upright'' (Table 2). Two sizes of silver NPs, 5 nm and 25 nm CMD were used. In addition, agglomerates of 250 nm CMD derived from 5 nm or 25 nm silver NPs were modeled using a density of a loosest packing of spherical silver NPs of $\rho_{wp} = 5.49$ g/cm^3. To calculate the deposition of NPs of the precise diameter, the size distribution was set to GSD = 1.0, which simulates perfectly monodispersed NPs to increase comparability and to avoid ''contaminating'' the resulting deposition data with different sized particles. Two aerosol concentrations were considered: 0.000687 mg/m^3 corresponding to 1×10^6 particles/cm^3 of 5 nm CMD, and 0.0858 mg/m^3 corresponding to 1×10^6 particles/cm^3 with 25 nm CMD. Table 2 shows the deposition in the various respiratory tract regions relative to the inhaled dose, and the deposited mass per breath. The calculations show that 92.57% of the 5 nm NPs, 68.01% of the 25 nm NPs, and 29.13% of the 250 nm agglomerates are deposited in the respiratory tract (''head'', ''conducting airways'' and ''alveolar region'' altogether). The relative deposition in the respiratory tract as well as the distribution of the particles between the three

Table 1. Nanomaterial parameters used in the MPPD calculations (as requested in the MPPD menu Input Data > Particle Properties).

Material	Density (g/cm^3)	Density (loosest packing*) (g/cm^3)	Diameter (μm)	CMD/MMD/ MMAD	GSD (diam.)	Nanoparticle model	Inhalation adjustment
Silver	10.49		0.005	CMD	1.0	Yes	Yes
	10.49		0.025	CMD	1.0	Yes	Yes
		5.49	0.250	CMD	1.0	Yes	Yes
		5.49	0.250	CMD	2.0	Yes	Yes
	10.49	5.49	0.035	CMD	1.5	Yes	Yes
Zirconia	5.68	2.97	0.009	CMD	1.5	Yes	Yes
Silica	2.2	1.15	0.014	CMD	1.5	Yes	Yes

CMD, count median diameter; MMD, mass median diameter; MMAD, mass median aerodynamic diameter; GSD, geometric standard deviation; diam., diameter.

*For an explanation of loosest packing of spheres refer the section ''Materials and methods''.

Table 2. Calculation of the deposition per breath for different diameters of silver NPs using MPPD and the exposure scenario ''consumer upright''.

	Exposure dose (CMD, GSD = 1.0)					
	0.000687 mg/m^3			0.0858 mg/m^3		
Diameter	5 nm[a]	25 nm[a]	250 nm[b]	5 nm[a]	25 nm[a]	250 nm[b]
NPs/cm^3	1×10^6	8×10^3	15	125×10^6	1×10^6	1.9×10^3
Head						
(%)	44.6	11.6	13.3	44.6	11.6	13.3
(ng)	0.31	0.080	0.091	38	10	11
Conducting airways						
(%)	35.41	16.34	4.96	35.41	16.34	4.96
(ng)	0.24	0.11	0.034	30	14	4.3
Alveolar region						
(%)	12.56	40.07	10.87	12.56	40.07	10.87
(ng)	0.086	0.28	0.075	11	34	9.3
NPs/alveolar macrophage	0.02	0.0005	0.0000003	3	0.07	0.00004

CMD, count median diameter; GSD, geometric standard deviation.
[a]Density of solid material.
[b]Density of loosest packing of spheres (Table 1).

Table 3. Calculated mass and particle number corresponding to the human $NOEL_{hyp}$ derived by the overload volume of 1.5 μm^3 per alveolar macrophage for different NPs.

			Overload volume of 1.5 μm^3			
			Solid		Loosest packing*	
Material	CMD (nm)	Density (g/cm^3)	(pg)	Number	(pg)	Number
Silver	35	10.49	15.7	6.68×10^4	8.24	3.50×10^4
Zirconia	9	5.68	8.52	3.93×10^6	4.46	2.06×10^6
Silica	14	2.2	3.30	1.04×10^6	1.73	0.55×10^6
Boehmite	16	3.04	4.56	6.99×10^5	2.39	3.66×10^5
Titania	21	4.23	6.35	3.09×10^5	3.32	1.62×10^5
Zinc oxide	40	5.606	8.41	4.48×10^4	4.40	2.34×10^4
Barium sulfate	32	4.48	6.72	8.74×10^4	3.52	4.58×10^4

CMD, count median diameter.
The list includes additional materials used as reference materials in several programs with densities in the range of the three materials discussed in the text.
*For an explanation of loosest packing of spheres refer to ''Materials and methods'' section.

specified areas of the respiratory tract is the same for the two concentrations. In fact, MPPD uses a linear relation of the distribution; hence, the relative deposition between areas is independent of the dose for a given material.

Deposition increases with decreasing particle size in the tracheobronchial area (''conducting airways''). In the alveolar region, the 25 nm NPs exhibited the highest deposition, while 5 nm NPs and the less-dense 250 nm NPs show a similar fraction deposited. In addition, MPPD calculates the particle number per alveolar macrophage (Table 2). At the higher concentration, three particles of 5 nm are deposited per alveolar macrophage corresponding to a mass of 2 ag (attograms) and, assuming a perfectly smooth surface, a surface area of 236 nm^2. Of the 25 nm particles, 0.07 are deposited per alveolar macrophage corresponding to a higher mass of 6 ag and a smaller surface area of 137 nm^2. Thus, while a lower mass of the smaller NPs is deposited, a larger surface area is exposed.

Although it is controversial whether the overload effect occurs only in rats, the overload volume derived by Morrow (1988) may be calculated for human alveolar macrophages as well. Based on the volume of a human macrophage of about 2500 μm^3 and accepting the 6% threshold loading also for human alveolar macrophages as has been argued by Oberdörster (1995), the overload effect would occur at a chronic loading of 150 μm^3 per human alveolar macrophage. This value will be used as the hypothetical lowest observed effect level ($LOEL_{hyp}$). In order to use the values of the deposited particle mass calculated in MPPD and the derived particle volumes for risk estimation, a no observed effect level ($NOEL_{hyp}$) is extrapolated from the $LOEL_{hyp}$. For this purpose, two safety factors are introduced; a factor of ten to represent the variability within the population (intraspecies variability, the interspecies extrapolation being addressed by using the specific macrophage volume), and a second factor of ten for the extrapolation of LOEL to NOEL. Hence, the overload hypothesis in humans postulates a $NOEL_{hyp}$ of 1.5 μm^3 deposition per alveolar macrophage. MPPD calculates the deposition by mass and particle number per alveolus and per alveolar macrophage. Knowing the density and the diameter of each material, the corresponding mass and particle number can be determined. Since the packing of particles affects the density of agglomerates, the calculated mass and number of some nanomaterials constituting the $NOEL_{hyp}$ are given in Table 3 for a perfect packing and for the loosest packing of spherical particles.

MPPD allows the graphical representation of the size-dependent deposition in three compartments of the respiratory tract. Sizes from 0.001 to 10 μm were used for the deposition as shown in Figure 1. MPPD has a fixed setting of CMD, and GSD = 1.0 for these calculations. Note that, as mentioned above, MPPD uses a dose-independent linear relationship of the distributions. MPPD calculates the relative deposition in the head, the

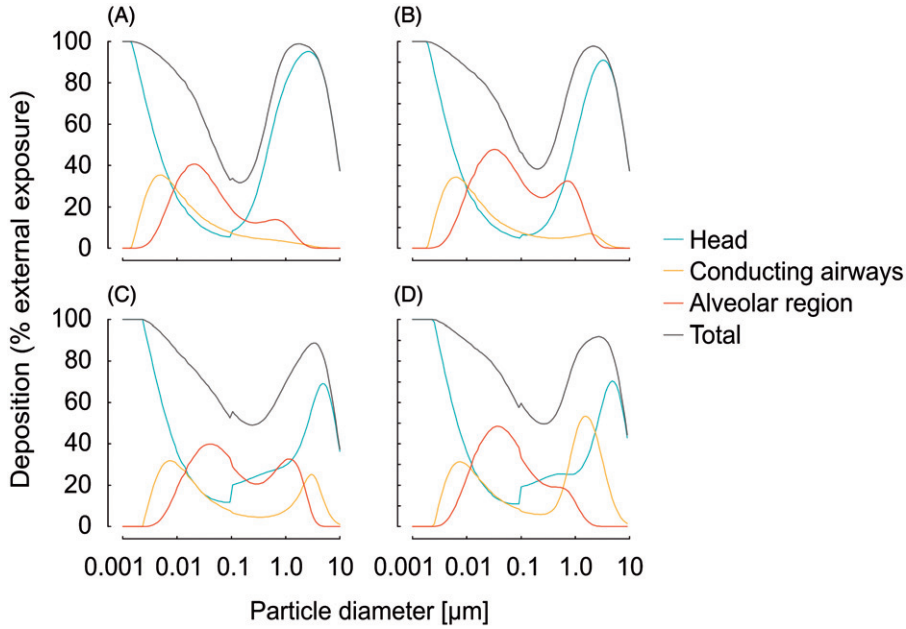

Figure 1. Relative deposition of silver (% external exposure) against particle diameter [µm] for the four exposure scenarios as calculated by MPPD. Note that the exposure dose has no influence on the relative distribution in MPPD v2.11. (A) Consumer, upright; (B) consumer, leaning forward; (C) bystander, child; (D) infant, lying. Total deposition (black), head (middle gray, blue), conducting airways (light gray, yellow), alveolar region (dark gray, red).

Table 4. Mass deposition of NPs per alveolar macrophage upon exposure to 1.10^6 particles/cm^3 for 5 min.

	35 nm Silver NPs		9 nm Zirconia NPs		14 nm Silica NPs	
	Deposition (fg)	Difference to $NOEL_{hyp}$	Deposition (fg)	Difference to $NOEL_{hyp}$	Deposition (fg)	Difference to $NOEL_{hyp}$
Consumer, upright	1.07	7 717	0.0126	354 549	0.0194	89 829
Consumer, leaning forward	0.913	9 029	0.00729	612 202	0.0127	136 432
Bystander, child	0.455	18 127	0.00299	1 492 754	0.00558	311 368
Infant, lying	0.590	13 971	0.00729	612 202	0.00956	181 806

The difference to $NOEL_{hyp}$ was calculated using the values from Table 3 and describes the number of exposures needed to reach overload conditions (288 exposures of 5 min each = 24 h).

conducting airways (tracheobronchial region), and in the alveolar region. Figure 1 compares the relative deposition of silver particles for the four exposure scenarios (see Supplemental Figures 1 and 2 for zirconia and silica particles, respectively). Overall, the four exposure scenarios show similar distributions. Particles in the nanoscale range deposit especially in the head and tracheobronchial area, larger nanoscale particles deposit mainly in the alveolar region, and a much lower deposition of particles with micrometer diameter is observed in the alveolar region. However, the age-specific 5-Lobe lung model (Figures 1B–D) shows a somewhat greater deposition of microscale particles in the alveolar region and less in the head portion than the default ''Yeh-Schum 5-Lobe'' lung model, which was used for the ''consumer, upright'' scenario (Figure 1A). In the scenarios using the ''Age-specific 5-Lobe'' lung model for the ages of 3 months or 3 years, additional deposition of microscale particles in the tracheobronchial area is observed (Figures 1C–D) (see also Asgharian et al., 2004).

For an exposure estimation of the silver, silica and zirconia materials, an aerosol concentration of 1×10^6 particles/cm^3 was assumed. A low rate of agglomeration is expected at this concentration. Thus, deposition and the resulting overload can be exclusively ascribed to nanoscale materials under these conditions. The corresponding concentrations were then used in the four exposure scenarios. Only deposition is considered and, as a worst case, summed up for the duration of exposure. MPPD calculates the deposition per breath, and the number of breaths per minute for each scenario can be found in Supplemental Tables 1–4. For all exposure situations a five-minute exposure is assumed. This comprises the dwell time in the spray cloud, meaning the spraying as well as following actions. Depositions for the different materials are shown in Table 4. The number of applications required to reach the $NOEL_{hyp}$ without accounting for clearance were calculated from the values given in Table 3.

The highest lung burden after a single use of five minutes is reached in the exposure scenario ''consumer, upright'' using a silver NP-containing spray (Table 4). The deposited amount is also closest to the human $NOEL_{hyp}$. Under this scenario, and ignoring clearance, 7717 applications are required to reach the value of the $NOEL_{hyp}$.

Furthermore, a high-dosed spray was modeled based on doses and particle size distributions reported for some consumer sprays (Quadros & Marr, 2011) as well as high dose experiments on rats (Landsiedel et al., 2010, 2014). For the NPs a dose equivalent to 1×10^8 particles/cm^3 of the respective NP at an agglomerated state of CMD = 250 nm and a GSD = 2.0 (corresponding to 2.476 µm MMAD) was assumed. Therefore, the density of the loosest packing (Table 1) was used to simulate stable agglomerates. Table 5 lists the deposition and the difference to the $NOEL_{hyp}$ for three different materials. These conditions lead to the highest deposition of 53.9 fg (femtograms) per alveolar macrophage in 5 min using a silver NP spray in the scenario ''infant, lying''. This scenario yields the highest deposition under these conditions because the Age-specific 5-Lobe lung model

Table 5. Mass deposition of NPs per alveolar macrophage upon exposure to $1{\cdot}10^8$ particles/cm^3 of agglomerates of 250 nm CMD, GSD = 2.0, of the density of the loosest packing for 5 min.

	Silver NPs		Zirconia NPs		Silica NPs	
	deposition [fg]	difference to $NOEL_{hyp}$	deposition [fg]	difference to $NOEL_{hyp}$	deposition [fg]	difference to $NOEL_{hyp}$
Consumer, upright	37.5	219	0.359	12 439	0.473	3652
Consumer, leaning forward	51.6	160	0.487	9163	0.621	2783
Bystander, child	31.2	264	0.265	16 806	0.312	5530
Infant, lying	53.9	153	0.570	7831	0.856	2019

The difference to $NOEL_{hyp}$ was calculated using the values from Table 3 and describes the number of exposures needed to reach overload conditions (288 exposures of 5 min each = 24 h).

(Figure 1B, C and D) has a higher fraction of large particles reaching the alveoli than the Yeh-Schum 5-Lobe lung model (Figure 1A), which showed the highest deposition for the smaller particles, and because of the mouth breathing of the infant. Calculated by the deposited mass, 229 silver NPs of 35 nm are deposited per alveolar macrophage at a concentration of 1×10^8 particles/cm^3 in five minutes. Overload conditions would be reached after 153 applications, or 12.7 hours of continuous exposure, again by neglecting clearance.

Discussion

Nanomaterials in spray applications remain a concern for human health because of their possible access to the distal parts of the lung. We used MPPD to model different exposure scenarios for the consumer.

First, the internal exposure by silver NPs of three different sizes was investigated. In addition to 5 and 25 nm particles, we modeled 250 nm agglomerates derived from 5 nm or 25 nm silver NPs. Since we used the simple approach to mathematically assign a reduced, so called ''loosest packing'' density to the latter particles, the actual size of the original particles in this agglomerate is inconsequential for the calculations. Two different doses by particle number of NPs were entered (Table 2). With about 93%, nearly all of the 5 nm NPs get deposited in the respiratory tract. While more than two-thirds of the 25 nm NPs with 68% deposit in the respiratory tract, less than one-third (29%) of 250 nm agglomerates are retained. It is important to note that the relative deposition is independent of the dose in the MPPD model. When these fractions are transformed into deposited mass, at the same particle number of 1×10^6 particles/cm^3 a much higher mass of 25 nm NPs of 58 ng is deposited compared to 0.64 ng of 5 nm NPs (sums of the respective columns in Table 2). Similarly, upon formation of 250 nm agglomerates derived from 1×10^6 particles/cm^3 of 5 nm NPs only 0.20 ng deposit, while of 250 nm agglomerates derived from 1×10^6 particles/cm^3 of 25 nm NPs 25 ng deposit (sums of the respective columns in Table 2). However, the calculated alveolar deposition at 1×10^6 particles/cm^3 exposure is two particles of 5 nm NPs versus seven particles of 25 nm NPs per 100 macrophages per breath (Table 2). Several studies have indicated a positive correlation of particle surface area with the toxicity of nanomaterials (Hansen & Baun, 2012). At the same particle number exposure, the exposed surface of 25 nm NPs would be 87-fold higher than that of the 5 nm NPs. Conversely, at the same mass concentration, the number and surface area of ingested 5 nm NPs compared to 25 nm NPs would be higher by more than 40-fold and 60%, respectively. Interestingly, our calculations regarding the 250 nm agglomerates of about 11% deposition in the alveolar region lie within those previously modeled for cosmetic powder (Nazarenko et al., 2012b).

We modeled a propellant spray for different NPs with low agglomeration and exposure of consumers in different scenarios in MPPD (Table 4). The highest deposition in mass is found for the larger and denser silver NPs. Furthermore, of the four tested scenarios ''consumer, upright'' exhibits the highest mass deposition per alveolar macrophage. Main contributors are the large tidal volume and the higher respiratory rate in this scenario. In addition, the large primary diameter of the silver NPs compared to the other nanomaterials investigated here is of influence. The average number of NPs per alveolar macrophage is similar for silver (35 nm), silica (14 nm) and zirconia (9 nm) with five, six and six particles, respectively. Clearly, the rate of uptake of NPs by macrophages depends on their diameter and is also influenced by a number of additional factors, such as surface modifications (Kettler et al., 2014). We compared our results to a hypothetical human $NOEL_{hyp}$ derived from the overload hypothesis formulated by Morrow (1988). Using the calculated values at which the $NOEL_{hyp}$ is reached for the different NPs (Table 3), we found that at the highest exposure scenario of ''consumer, upright'' with silver NPs, the modeled spray application would have to be repeated over a period of about 21 years (i. e. 7717 times 5 min applications) to reach the value of the $NOEL_{hyp}$ (Table 4). In the case of continuous exposure, exposure would have to last for 26.8 days. It is to be expected that clearance will significantly reduce the particle load over this longer period, and the overload scenario refers to a chronic exposure. Thus, overload conditions are not achieved under the chosen conditions.

In addition, we modeled the exposure to a high concentration spray. As the high dose of 1×10^8 particles/cm^3 agglomerates with a broad size distribution were assumed (Table 5), the parameters were similar to high-dose exposures in *in vivo* inhalation experiments (Landsiedel et al., 2010, 2014). Here, the highest exposure was with silver NPs and the scenario ''infant, lying''. The Age-specific 5-Lobe lung model (Figure 1B, C and D) and an oronasal-mouth breather estimate a higher fraction of larger particles reaching the alveoli compared to the Yeh-Schum 5-Lobe lung model (Figure 1A). Moreover, in the case of ''infant, lying'' (Figure 1D), mouth breathing was assumed resulting in an even larger fraction of the micrometer-sized particles reaching the conducting airways and of nanometer-sized particles reaching the alveolar region compared to the oronasal-mouth breather ''bystander, child'' (Figure 1C). Overload conditions would be reached after 153 five-min applications, or 12.7 h of continuous exposure. Excessive and daily use could therefore potentially lead to overload conditions and chronic exposure. For the smaller and lighter silica or zirconia NPs, overload conditions are reached only after several thousands of five-min applications. As discussed earlier, our calculations ignore the clearance mechanism of the lung and are thus gross overestimations of chronically deposited material, rendering the overload condition even less likely. However, potential chemical specific inherent toxicity of

NPs, such as genotoxicity as observed for silver, copper oxide and zinc oxide nanomaterials *in vitro* (Magdolenova et al., 2014) always has to be considered in a weight of evidence approach. This will render the overload hypothesis obsolete for risk management decisions for such materials.

According to the World Health Organization (WHO), there is no fine dust concentration below which no adverse effect is expected (WHO, 2014). Consequently, European legislation limited the environmental exposure to ultra fine particles (particulate matter PM 2.5) to 25 $\mu g/m^3$ as yearly average legally by 2015, and to 20 $\mu g/m^3$ starting by 2020. In some German cities, average environmental levels were above 20 $\mu g/m^3$ in the year 2013 (UBA, 2014). Under the conditions of a daily 5 min use of the propellant spray, the high-dose silver NP spray would create an exposure above these environmental levels of 82 $\mu g/m^3$ averaged over the day. All other scenarios have doses of at least 75-fold less and thus contribute little to general exposure. Although this apparently gives the all-clear for low-dose NPs in consumer spray applications, we assumed the particles to be biopersistent and inert as required in the overload hypothesis (Morrow, 1988). It should be noted that the term biopersistent is currently not well defined even though some legal texts already incorporate it into their definition of nanomaterial, such as the regulation No 1223/2009 of the European parliament and of the council of 30 November 2009 on cosmetic products. However, for most materials, material-specific effects must be considered. We will therefore briefly discuss some effects pertaining to the materials used in this study. No acute toxicity by inhalation of silver NP with concentrations of 9.4×10^5 to 3.08×10^6 particles/cm^3 was found (Sung et al., 2011). In a subacute repeated dose study, silver NPs were utilized at concentrations ranging from 1.7×10^4 to 1.3×10^6 particles/cm^3 (Ji et al., 2007). At the highest dose, increased blood calcium was found, but no adverse effect could be assigned to these observations. In a subchronic repeated dose study, silver NPs with concentrations of 6.6×10^5 to 2.9×10^6 particles/cm^3 were investigated (Sung et al., 2008). At the highest dosage, changes in lung function and histopathological changes in the lung tissue were detected (Sung et al., 2008). A more detailed analysis of the data revealed bile duct hyperplasia at the highest dose (Sung et al., 2009). An analog calculation to the one presented in this study, of these data for rat, demonstrated that overload conditions would be reached after nearly four weeks of exposure (Riebeling & Kneuer, 2014). Thus, under the worst-case scenario of no clearance, the observed effects coincide with overload conditions. Another follow-up study found no significant increase in multinucleated polychromatic erythrocytes in bone marrow (Kim et al., 2011). However, it should be noted that the presence of silver in bone marrow was not determined in the study and data for intravenous injection show clear genotoxic effects of silver NPs (Dobrzynska et al., 2014). A study investigating the reversibility of lung function showed impairment after 12 weeks of exposure employed silver NPs with concentrations of 6.6×10^5 to 3.2×10^6 particles/cm^3 (Song et al., 2013). At the highest dose, some lung inflammation was detected even after 12 weeks of follow-up indicating possible chronic damage.

The overload hypothesis applies best to zirconia because it is of very low reactivity, almost insoluble in water, and no toxicologically relevant effects of the bulk material have been reported. Micrometer scale particles have been investigated for inhalation (Mohr et al., 2006; Pott & Roller, 2005), and zirconia NPs at high-dose in agglomerated state (Landsiedel et al., 2010). In the nanoGEM project, two surface-modified zirconia nanomaterials were tested in animal short-term inhalation studies (Landsiedel et al., 2014). No abnormalities in the investigated endpoints or health effects were found using doses of 2–50 mg/m^3, with strong agglomeration with an average diameter of the particles in the aerosol of 0.37 to 1.4 µm.

A similar situation exists for amorphous silica. Many studies are using the NPs at a high-dose, which results in strong agglomeration in the micrometer range (Landsiedel et al., 2010; Reuzel et al., 1991), and thus it is unclear if they are representative for exposure to NPs as such. In the nanoGEM project, four surface-modified silica nanomaterials were tested in animal short-term inhalation studies (Landsiedel et al., 2014). Here, no abnormalities in the investigated endpoints or health effects were found using doses of 2–50 mg/m^3. Strong agglomeration occurred, so that the diameter of the particles in the aerosol was 0.7–2.0 µm. The concentrations used for zirconia and silica by Landsiedel et al. (2014) were far higher than in the above discussed study of silver (Riebeling & Kneuer, 2014; Sung et al., 2009), likely inducing overload conditions. However, exposure times were shorter which precludes a direct comparison.

Moreover, silver NPs and silica NPs can act as adjuvants when administered intraperitoneally (Brandenberger et al., 2013; Xu et al., 2013). However, there is no conclusive evidence whether free NPs pass into the bloodstream after inhalation and are able to trigger immunostimulatory effects by this route. Since NPs may act as adjuvant, and also might act as a vehicle, carrying allergens deep into the lungs, they represent a possible enhancer of asthmatic diseases. As part of the nanoGEM project, various silica NP were instilled in ovalbumin-sensitized mice, which represents an asthma model (Marzaioli et al., 2014). An increase in neutrophils was demonstrated in the alveolar fluid in ovalbumin-sensitized as well as in non-sensitized animals, influenced by the NPs' surface modification. Instillation increased pulmonary inflammation and generally led to a goblet cell necrosis (Marzaioli et al., 2014). Tests of lung function, however, showed only moderate adverse effects of the instillation. These data indicate possible immunological effects of NPs.

In addition to the specific material properties, as suggested by the ''Magic Nano'' spray incident (Pauluhn et al., 2008), chemicals might adsorb to the surface of nanomaterials. In the case of the lung, even inert NPs thereby could function as carriers of chemicals deep into the lung. Hence, by this mechanism, a product formulation using individually safe ingredients may become a hazard. Based on this reasoning, nanomaterials in propellant spray applications still remain a concern for consumer safety.

Acknowledgements

We would like to thank Anja Köth, Heinz Kaminski and Thomas Kuhlbusch for their involvement in research leading up to data related but not discussed in this study.

Declaration of interest

The authors declare no conflict of interest.

This study was supported by the German Federal Ministry of Education BMBF, nanoGEM Project, FKZ 03X0105. Parts of the data have been discussed and are published in the final report of the nanoGEM project (see: www.nanogem.de).

References

Altman PL, Dittmer Katz D. 1971. Respiration and Circulation. Bethesda, MD: Federation of American Societies for Experimental Biology.

Anjilvel S, Asgharian B. 1995. A multiple-path model of particle deposition in the rat lung. Fundam Appl Toxicol 28:41–50.

Asgharian B, Menache MG, Miller FJ. 2004. Modeling age-related particle deposition in humans. J Aerosol Med 17:213–24.

Balasubramanian SK, Poh KW, Ong CN, Kreyling WG, Ong WY, Yu LE. 2013. The effect of primary particle size on biodistribution of inhaled gold nano-agglomerates. Biomaterials 34:5439–52.

BfR. 2006. Nano particles were not the cause of health problems triggered by sealing sprays! Press Releases of the German Federal Institute for Risk Assessment [Online]. Available at: http://www.bfr.bund.de/en/press_information/2006/12/nano_particles_were_not_the_cause_of_health_problems_triggered_by_sealing_sprays_-7842.html. Accessed on 15 January 2015.

Brandenberger C, Rowley NL, Jackson-Humbles DN, Zhang Q, Bramble LA, Lewandowski RP, et al. 2013. Engineered silica nanoparticles act as adjuvants to enhance allergic airway disease in mice. Part Fibre Toxicol 10:26. doi: 10.1186/1743-8977-10-26.

Chen BT, Afshari A, Stone S, Jackson M, Schwegler-Berry D, Frazer DG, et al. 2010. Nanoparticles-containing spray can aerosol: characterization, exposure assessment, and generator design. Inhal Toxicol 22: 1072–82.

Dobrzynska MM, Gajowik A, Radzikowska J, Lankoff A, Dusinska M, Kruszewski M. 2014. Genotoxicity of silver and titanium dioxide nanoparticles in bone marrow cells of rats in vivo. Toxicology 315: 86–91.

Dunnill MS. 1962. Postnatal growth of the lung. Thorax 17:329–33.

Gomez V, Levin M, Saber AT, Irusta S, Dal Maso M, Hanoi R, et al. 2014. Comparison of dust release from epoxy and paint nanocomposites and conventional products during sanding and sawing. Ann Occup Hyg 58:983–94.

Hagendorfer H, Lorenz C, Kaegi R, Sinnet B, Gehrig R, von Goetz N, et al. 2010. Size-fractionated characterization and quantification of nanoparticle release rates from a consumer spray product containing engineered nanoparticles. J Nanopart Res 12:2481–94.

Hansen SF, Baun A. 2012. European regulation affecting nanomaterials – review of limitations and future recommendations. Dose Response 10: 364–83.

Hart MC, Cook CD, Orzalesi MM. 1963. Relation between anatomic respiratory dead space and body size and lung volume. J Appl Physiol 18:519–22.

Hofmann W. 1982. Mathematical model for the postnatal growth of the human lung. Respir Physiol 49:115–29.

Ji JH, Jung JH, Kim SS, Yoon JU, Park JD, Choi BS, et al. 2007. Twenty-eight-day inhalation toxicity study of silver nanoparticles in Sprague-Dawley rats. Inhal Toxicol 19:857–71.

Kalberlah F, Schneider K, Schuhmacher-Wolz U. 2011. Gutachten zur biologischen Plausibilität von HEC und MPPD [Online]. Freiburg: German Federal Institute for Occupational Safety and Health (BAuA). Available at: http://www.baua.de/de/Themen-von-A-Z/Gefahrstoffe/TRGS/pdf/Gutachten-HEC-MPPD.pdf?__blob=publicationFile&v=1. Accessed on 26 July 2013.

Kendall M, Holgate S. 2012. Health impact and toxicological effects of nanomaterials in the lung. Respirology 17:743–58.

Kettler K, Veltman K, van de Meent D, van Wezel A, Hendriks AJ. 2014. Cellular uptake of nanoparticles as determined by particle properties, experimental conditions, and cell type. Environ Toxicol Chem 33: 481–92.

Kim JS, Sung JH, Ji JH, Song KS, Lee JH, Kang CS, Yu IJ. 2011. In vivo genotoxicity of silver nanoparticles after 90-day silver nanoparticle inhalation exposure. Saf Health Work 2:34–8.

Kreyling WG, Hirn S, Möller W, Schleh C, Wenk A, Celik G, et al. 2014. Air-blood barrier translocation of tracheally instilled gold nanoparticles inversely depends on particle size. ACS Nano 8:222–33.

Labouta HI, Schneider M. 2013. Interaction of inorganic nanoparticles with the skin barrier: current status and critical review. Nanomedicine 9:39–54.

Landsiedel R, Ma-Hock L, Hofmann T, Wiemann M, Strauss V, Treumann S, et al. 2014. Application of short-term inhalation studies to assess the inhalation toxicity of nanomaterials. Part Fibre Toxicol 11:16. doi: 10.1186/1743-8977-11-16.

Landsiedel R, Ma-Hock L, Kroll A, Hahn D, Schnekenburger J, Wiench K, Wohlleben W. 2010. Testing metal-oxide nanomaterials for human safety. Adv Mater 22:2601–27.

Lewinson J, Mayr W, Wagner H. 1994. Characterization and toxicological behavior of synthetic amorphous hydrophobic silica. Regul Toxicol Pharmacol 20:37–57.

Lorenz C, Hagendorfer H, von Goetz N, Kaegi R, Gehrig R, Ulrich A, et al. 2011. Nanosized aerosols from consumer sprays: experimental analysis and exposure modeling for four commercial products. J Nanopart Res 13:3377–91.

Magdolenova Z, Collins A, Kumar A, Dhawan A, Stone V, Dusinska M. 2014. Mechanisms of genotoxicity. A review of in vitro and in vivo studies with engineered nanoparticles. Nanotoxicology 8:233–78.

Martin KR. 2007. The chemistry of silica and its potential health benefits. J Nutr Health Aging 11:94–7.

Marzaioli V, Aguilar-Pimentel JA, Weichenmeier I, Luxenhofer G, Wiemann M, Landsiedel R, et al. 2014. Surface modifications of silica nanoparticles are crucial for their inert versus proinflammatory and immunomodulatory properties. Int J Nanomed 9:2815–32.

McKinney W, Jackson M, Sager TM, Reynolds JS, Chen BT, Afshari A, et al. 2012. Pulmonary and cardiovascular responses of rats to inhalation of a commercial antimicrobial spray containing titanium dioxide nanoparticles. Inhal Toxicol 24:447–57.

Mohr U, Ernst H, Roller M, Pott F. 2006. Pulmonary tumor types induced in Wistar rats of the so-called ''19-dust study''. Exp Toxicol Pathol 58: 13–20.

Morrow PE. 1988. Possible mechanisms to explain dust overloading of the lungs. Fundam Appl Toxicol 10:369–84.

Mortensen JD, Stout L, Bagley B, Burkart J, Schaap RN. 1989. Age related morphometric analysis of human lung casts. In: Crapo JD, Miller FJ, Graham J, Hayes A, eds. Extrapolation of Dosimetric Relationships for Inhaled Particles and Gases. San Diego, CA: Academic Press, 59–68.

Mortensen JD. 1983. A Study of Age Specific Human Respiratory Morphometry: Final Report. Salt Lake City, Utah: UBTL Division, University of Utah Research Institute.

Nazarenko Y, Han TW, Lioy PJ, Mainelis G. 2011. Potential for exposure to engineered nanoparticles from nanotechnology-based consumer spray products. J Expo Sci Environ Epidemiol 21:515–28.

Nazarenko Y, Zhen H, Han T, Lioy PJ, Mainelis G. 2012a. Nanomaterial inhalation exposure from nanotechnology-based cosmetic powders: a quantitative assessment. J Nanopart Res 14:1229. doi: 10.1007/s11051-012-1229-2.

Nazarenko Y, Zhen H, Han T, Lioy PJ, Mainelis G. 2012b. Potential for inhalation exposure to engineered nanoparticles from nanotechnology-based cosmetic powders. Environ Health Perspect 120:885–92.

Nohynek GJ, Dufour EK. 2012. Nano-sized cosmetic formulations or solid nanoparticles in sunscreens: a risk to human health? Arch Toxicol 86:1063–75.

Oberdörster G. 1995. Lung particle overload: implications for occupational exposures to particles. Regul Toxicol Pharmacol 21:123–35.

Overton JH, Graham RC. 1989. Predictions of ozone absorption in human lungs from newborn to adult. Health Phys 57:29–36.

Pauluhn J, Hahn A, Spielmann H. 2008. Assessment of early acute lung injury in rats exposed to aerosols of consumer products: attempt to disentangle the ''Magic Nano'' conundrum. Inhal Toxicol 20:1245–62.

Peters R, Kramer E, Oomen AG, Rivera ZE, Oegema G, Tromp PC, et al. 2012. Presence of nano-sized silica during in vitro digestion of foods containing silica as a food additive. ACS Nano 6:2441–51.

Phalen RF, Oldham MJ, Beaucage CB, Crocker TT, Mortensen JD. 1985. Postnatal enlargement of human tracheobronchial airways and implications for particle deposition. Anat Rec 212:368–80.

Pott F, Roller M. 2005. Carcinogenicity study with nineteen granular dusts in rats. Eur J Oncol 10:249–81.

Quadros ME, Marr LC. 2011. Silver nanoparticles and total aerosols emitted by nanotechnology-related consumer spray products. Environ Sci Technol 45:10713–19.

Reuzel PG, Bruijntjes JP, Feron VJ, Woutersen RA. 1991. Subchronic inhalation toxicity of amorphous silicas and quartz dust in rats. Food Chem Toxicol 29:341–54.

Riebeling C, Kneuer C. 2014. Challenges in human health hazard and risk assessment of nanoscale silver. In: Wohlleben W, Kuhlbusch T, Lehr CM, Schnekenburger J, eds. Safety of Nanomaterials Along Their Lifecycle: Release, Exposure and Human Hazards. New York: Taylor & Francis–Oxford, 417–35.

Skocaj M, Filipic M, Petkovic J, Novak S. 2011. Titanium dioxide in our everyday life: is it safe? Radiol Oncol 45:227–47.

Song KS, Sung JH, Ji JH, Lee JH, Lee JS, Ryu HR, et al. 2013. Recovery from silver-nanoparticle-exposure-induced lung inflammation and lung function changes in Sprague Dawley rats. Nanotoxicology 7:169–80.

Sung JH, Ji JH, Park JD, Yoon JU, Kim DS, Jeon KS, et al. 2009. Subchronic inhalation toxicity of silver nanoparticles. Toxicol Sci 108: 452–61.

Sung JH, Ji JH, Song KS, Lee JH, Choi KH, Lee SH, Yu IJ. 2011. Acute inhalation toxicity of silver nanoparticles. Toxicol Ind Health 27: 149–54.

Sung JH, Ji JH, Yoon JU, Kim DS, Song MY, Jeong J, et al. 2008. Lung function changes in Sprague-Dawley rats after prolonged inhalation exposure to silver nanoparticles. Inhal Toxicol 20:567–74.

UBA. 2014. Jährliche Auswertung Feinstaub (PM2,5) - 2013. Feinstaub - Jährliche Auswertungen [Online]. Available at: http://www.umweltbundesamt.de/sites/default/files/medien/358/dokumente/pm2_2013.pdf. Accessed on 15 January 2015.

Weir A, Westerhoff P, Fabricius L, Hristovski K, von Goetz N. 2012. Titanium dioxide nanoparticles in food and personal care products. Environ Sci Technol 46:2242–50.

WHO. 2014. Ambient (outdoor) air quality and health, Fact sheet N°313. Fact sheets [Online]. Available at: http://www.who.int/mediacentre/factsheets/fs313/en/. Accessed on 15 January 2015.

Wohlleben W, Kuhlbusch T, Lehr CM, Schnekenburger J. 2014. Safety of Nanomaterials Along Their Lifecycle: Release, Exposure and Human Hazards. New York: Taylor & Francis-Oxford, 1–472.

Xu Y, Tang H, Liu JH, Wang H, Liu Y. 2013. Evaluation of the adjuvant effect of silver nanoparticles both in vitro and in vivo. Toxicol Lett 219:42–8.

Yeh HC, Schum GM. 1980. Models of human lung airways and their application to inhaled particle deposition. Bull Math Biol 42:461–80.

Supplementary material available online

Supplementary Tables 1, 2, 3 and 4, Figures 1 and 2.